university of groningen

University Medical Center Groningen

University of Groningen

Electron transport across complex oxide heterointerfaces

Rana, Kumari Gaurav

IMPORTANT NOTE: You are advised to consult the publisher's version (publisher's PDF) if you wish to cite from it. Please check the document version below.

Document Version
Publisher's PDF, also known as Version of record

Publication date:
2013

Link to publication in University of Groningen/UMCG research database

Citation for published version (APA):
Rana, K. G. (2013). *Electron transport across complex oxide heterointerfaces*. s.n.

Copyright
Other than for strictly personal use, it is not permitted to download or to forward/distribute the text or part of it without the consent of the author(s) and/or copyright holder(s), unless the work is under an open content license (like Creative Commons).

The publication may also be distributed here under the terms of Article 25fa of the Dutch Copyright Act, indicated by the “Taverne” license. More information can be found on the University of Groningen website: https://www.rug.nl/library/open-access/self-archiving-pure/taverne-amendment.

Take-down policy
If you believe that this document breaches copyright please contact us providing details, and we will remove access to the work immediately and investigate your claim.

Downloaded from the University of Groningen/UMCG research database (Pure): http://www.rug.nl/research/portal. For technical reasons the number of authors shown on this cover page is limited to 10 maximum.

Download date: 04-06-2022

Chapter 7

Spin dependent transport across oxide multilayers

In this chapter we present our initial measurements of tunnel magnetoresistance (TMR) across $La_{0.67}Sr_{0.33}MnO_3/SrTiO_3/La_{0.67}Sr_{0.33}MnO_3$ *magnetic tunnel junctions (MTJ). Here,* $La_{0.67}Sr_{0.33}MnO_3$ *(LSMO) is used as the ferromagnetic (FM) electrodes and* $SrTiO_3$ *(STO) is used as a tunnel barrier. Co is deposited on top of the LSMO top electrode to enhance its coercivity by direct ferromagnetic coupling. The spin polarization (SP) of LSMO is quantified using Julliere's model. First, we present the fabrication steps that are performed to structure the multilayer stacks into magnetic tunnel junctions and is followed by its characterization, viz. electrical characterization of the junction, temperature and bias dependence of the TMR. Quantification of SP using MTJ is an important step towards the study of magnetic tunnel transistors.*

7.1 Magnetic tunnel junctions based on manganite

Magnetic tunnel junctions are relevant for the study of spin dependent electron transport and for their applications in information storage. They are being used as read heads of hard disk drivers and magnetoresistive random access memories (MRAM). A magnetic tunnel junction (MTJ) consists of two ferromagnetic conducting electrodes separated by an insulating thin layer. The tunneling probability between the two ferromagnetic electrodes is influenced by the spin polarization (SP) of the ferromagnetic layers as well as the tunneling property of the insulator, as illustrated in Fig. 7.1 [1], [2]. The high spin polarization in manganites and their high Curie temperature (above room temperature) classify them as one of the most promising candidates for ferromagnetic electrodes in MTJ. The use of LSMO as the ferromagnetic electrodes in MTJ, studied by Bowen et al. [3], showed a tunnel magnetoresistance (TMR) of 1800%; which has propelled a lot of research in this field. Such high values of TMR gave a spin polarization of nearly 95% in LSMO. Large TMR values have been measured in magnetic tunnel junctions using half-metallic manganites and various insulating thin barriers [4]-[9]. The interface between the ferromagnetic manganite and insulator plays an important role and dictates the

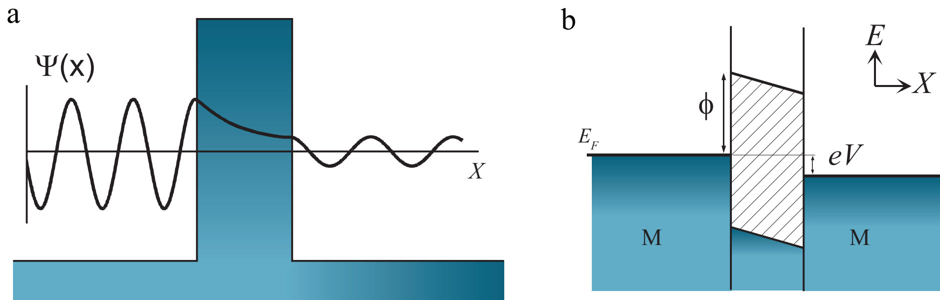

Figure 7.1: *(a) Schematic of an electron wavefunction tunneling between two metals (free electron model). (b) Schematic of a potential barrier separating two metals with a tunnel barrier. A bias voltage, V, is applied to one of the metals with respect to the other.*

value of magnetoresistance, hence interface engineering is one of the most promising ways of enhancing the TMR ratios in MTJ based on half-metallic manganites [11], [12].

7.1.1 Basic thoery of tunnel junctions

Metal/insulator/metal junction

When an external bias (V) is applied across the normal metal tunnel junction i.e. metal/insulator/metal (M/I/M), the Fermi levels of the electrodes shift by an amount of eV with respect to the other, as shown in Fig. 7.1. Taking a few simplified assumptions [10], the electron tunneling current I(E) at given energy E from the injecting electrode to the collecting electrode is:

$$I_{l\rightarrow r}(V) = \int_{-\infty}^{+\infty} \rho_1(E).\rho_r(E+eV)|M|^2 f(E)[1-f(E+eV)]dE \qquad (7.1)$$

where ρ(E) is the electrode density of states (DOS), f(E) is the Fermi-Dirac distribution and M(E,V) is the tunneling transfer matrix at energy E and applied bias V. Since the applied bias may involve new unoccupied states in the collecting electrode, and modify the potential profile of the barrier, this matrix element is energy- and bias-dependent [13].

The Julliere model

In 1975, Julliere proposed a simple phenomenological model in order to explain the TMR effect [14]. He proposed that the tunneling current for each spin direc-

tion is proportional to the product of the density of states at the Fermi level in the electrodes on both sides of the tunnel barrier. TMR is defined as a change in the resistance between the parallel and antiparallel states of magnetization of two ferromagnetic electrodes [14], i.e.:

$$TMR = \frac{R_{Antiparallel} - R_{Parallel}}{R_{Parallel}} \tag{7.2}$$

where, $R_{Parallel}$ is the resistance for the parallel alignment of magnetization (spins) of the electrodes and $R_{Antiparallel}$ is for the antiparallel condition. According to initial understanding of TMR (Tedrow and Mersevey [15]) the conduction electrons in ferromagnetic metals are spin polarized, and the spin is conserved in the tunneling process. Julliere's model, for FM/I/FM tunneling, predicts that the tunnel junction magnetoresistance depends on polarization of FM as:

$$TMR = \frac{2P_1P_2}{(1 - P_1P_2)} \tag{7.3}$$

where P_1 and P_2 are defined as the normalized difference between the density of states at the Fermi level for the majority and minority spin electrons. These polarizations are expressed as:

$$P_i = \frac{N_{i\downarrow}(E_F) - N_{i\uparrow}(E_F)}{N_{i\downarrow}(E_F) + N_{i\uparrow}(E_F)} \tag{7.4}$$

In this model, the spin polarization is an intrinsic property of the ferromagnetic material. In the case of a non magnetic electrode material, P = 0; and for a fully polarized condition on E_F, $|P|$ = 1. Julliere's model takes into account the spin dependent density of states only, but not the barrier/interface contributions.

In recent years, several modifications to these models have been proposed in order to include barrier effects and effective mass of the electron which depends on the actual band structure of the material, much in contrast to the free electron model assumed in Julliere's approach. From the Julliere's model, it immediately apparent that the materials with only one spin direction at the Fermi level (i.e. total spin polarization) should produce very high values of TMR. Half metallic manganites are hence the preferred candidates for oxide based spintronics.

7.2 Growth and fabrication of LSMO/$SrTiO_3$/LSMO magnetic tunnel junction

$La_{0.67}Sr_{0.33}MnO_3$ (LSMO) grows epitaxially on a $SrTiO_3$ substrate due to their low lattice mismatch. To ensure the epitaxy of the whole stack, $SrTiO_3$ is used as a tunnel

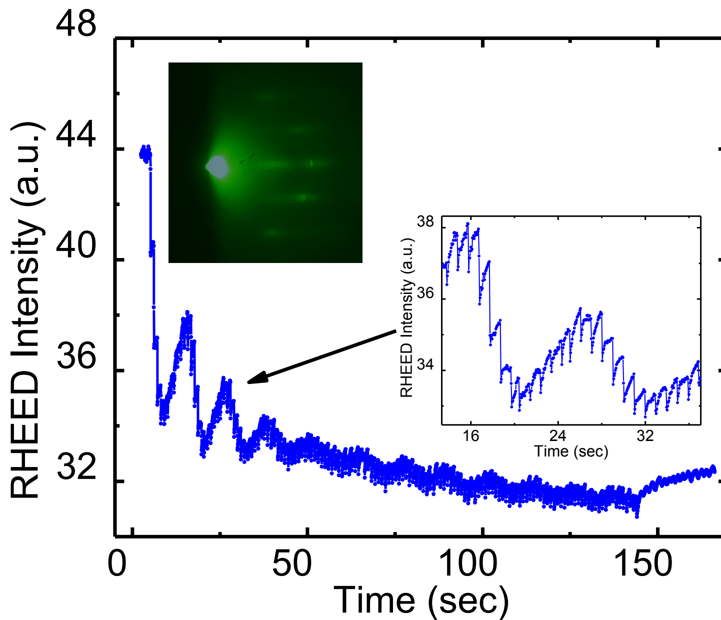

Figure 7.2: *RHEED intensity oscillation obtained during top layer ferromagnet (4.8 nm LSMO) growth using PLD on a (30nm)LSMO/(3nm)$SrTiO_3$ stack which is already grown on $SrTiO_3$ substrate.*

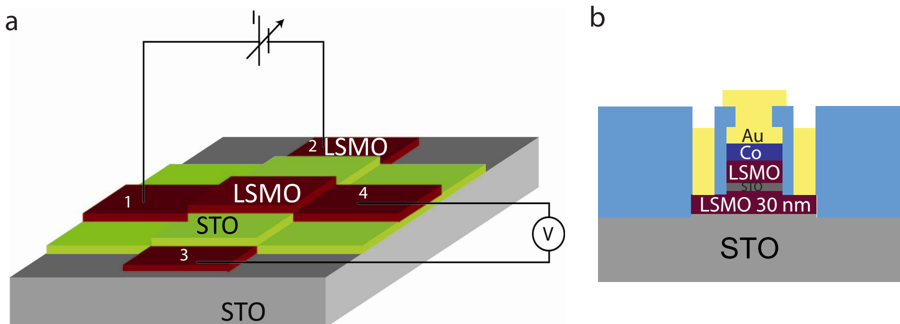

Figure 7.3: *Device schematics of the magnetic tunnel junction as well as the measurement scheme. A bottom ferromagnetic electrode and a top ferromagnetic electrode are separated by a thin $SrTiO_3$ tunnel barrier.*

barrier. The epitaxial barrier reduces the probability of defects or pinholes which are responsible for reducing the TMR or SP in MTJ.

A multilayer stack of LSMO/$SrTiO_3$/LSMO is epitaxially grown *in situ* using

PLD. Growth parameters for bottom and top ferromagnetic electrodes (LSMO) are kept the same as mentioned in chapter 2. For growing epitaxial $SrTiO_3$, we have used the similar growth parameters i.e. a temperature of 750°C and a deposition pressure of 0.35 mBar heater to target distance of 53 mm and laser fluence of 2.2 Jcm^{-2}. The growth of the multilayer stack is monitored using RHEED as explained earlier and is shown in Fig. 7.2. The left inset shows the RHEED spots after the whole multilayer stack is grown and the right inset shows the variation of RHEED spots during the growth of top layer LSMO electrode. Further, we also grew 10 nm thick film of Co on top of LSMO for enhancing the coercivity of top LSMO layer via direct ferromagnetic coupling and in order to protect the oxidation of Co, it is capped with 15 nm thin film of Au.

After growth of the multilayer, we fabricate magnetic tunnel junction devices using photo lithography and dry etching. The steps involved are explained in detail in chapter 2. We define ohmic contacts to the bottom LSMO bar and top ferromagnetic layer. We fabricate the device structures that allows us to measure four probe direct current (dc) electrical resistance of the magnetic tunnel junctions.

Figure 7.3 (a) shows a schematic view of the electrodes and the tunnel barrier. The $La_{0.67}Sr_{0.33}MnO_3$ bottom electrode has a rectangular shape of 3580×450 μm^2 area. The top electrode is elliptical. We use different sizes of the junctions with dimensions of of 30 by 50 μm^2 to 190 by 390 μm^2. There are 4 junctions in one LSMO bar and we have 4 such bars resulting in 16 MTJ devices on the single substrate. Figure 7.4 shows the optical microscope image of real tunnel junction device and wire bonded contacts for four probe measurements.

7.3 Electrical characterization of magnetic tunnel junctions

The results shown here are obtained from (15nm)Au/(10nm)Co/(4.8nm)LSMO/(3nm) $SrTiO_3$/(30nm)LSMO tunnel junction of size 100×200 μm^2 fabricated on $SrTiO_3$ substrate.

I-V of tunnel barrier

A four-point measurement configuration is used to measure the transport properties of the MTJ. The resistance of the LSMO bottom electrode is measured to be an order of magnitude smaller than that of the junction, hence we rule out artificial TMR due to other causes like inhomogeneous current injection [17]. The temperature dependence of the resistivity of similar thickness LSMO films is presented (section 4.5).

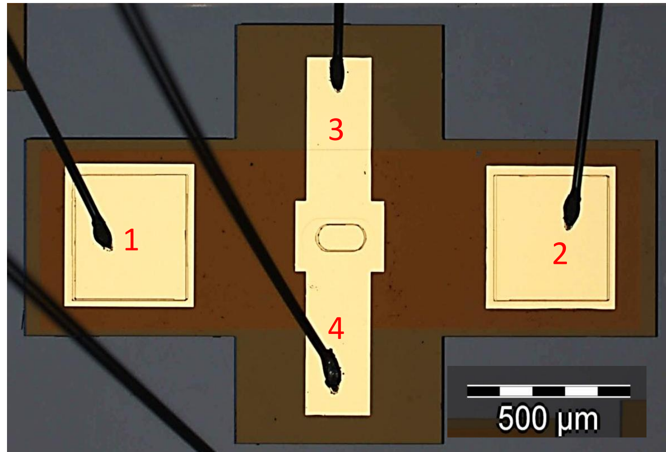

Figure 7.4: *Optical microscopic image of the real device where the wire bonded contacts are shown. 1 and 3 are used to source current to the junction whereas, 2 and 4 are used to measure the drop across junction (i.e using four probe geometry).*

Figure 7.5 shows two different current-voltage (I-V) characteristics of the MTJ, measured using four-probe geometry. A bias voltage of $\pm$125 mV is swept across the junction using contact 1 and 3 and the current is measured across 2 and 4. For the black curve (Parallel) a field of few 1000 Oe is applied to align the magnetization of both electrodes in a relatively parallel direction. In the other measurement (red curve) a field nearly 40 - 60 Oe,aligns the FM layers in antiparallel direction. We observe a non-linear I-V characteristics, typical of a tunnel barrier. Such characteristics indicate a tunnel barrier between the two ferromagnetic electrodes.

Magnetic field dependence

In Fig. 7.6, we show the magnetic field dependence of the junction resistance measured using four probe geometry. These measurements are performed at 68 K. A bias voltage of 1 mV is applied across the junction using contact 1 and 3 and the resistance is measured across 2 and 4. A magnetic filed is applied in a direction parallel to the bottom electrode LSMO (a rectangular bar). While sweeping the magnetic field from -3000 to +3000 Oe, the resistance of the junction rises from 255 kΩ to 345 kΩ, and its reversal back to -3000 Oe gives us almost similar change in the resistance. We use Eqn. 7.2 to calculate TMR and obtain a maximum of 14% TMR. Using Eqn. 7.3 and assuming $P = P_1 = P_2$ (for symmetric LSMO as ferromagnetic

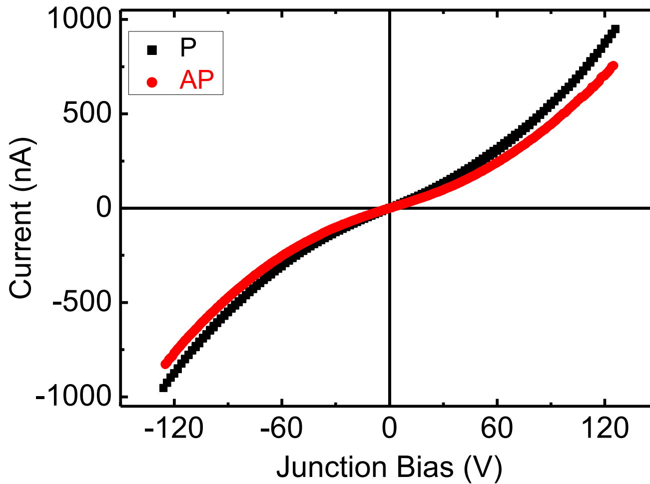

Figure 7.5: *Electrical characterization of tunnel barrier at 68 K. Four probe I-V characteristics for MTJ One curve is measured at an applied field of 3000 Oe when the magnetization of the layers is parallel. The other curve is measured at the high resistant state (antiparallel).*

electrodes), leads to a spin polarization of 36%.

Bias dependence of tunnel junction resistance

Figure 7.6 (a) shows the TMR values as a function of applied bias for the same junction, measured at 68K. A decrease in TMR as a function of applied bias is observed. Such a reduction in TMR could be caused by reduction in asymmetry of spin majority and minority as we go higher above the Fermi level. Another reason attributed to this is the interface magnon excitation [18]. The presence of defect states within the tunnel barrier may allow an increased amount of defect-state-assisted tunneling [19], and dilute the spin polarization of the tunneling current at elevated bias voltage [4], [20].

We have also obtained TMR values and its bias dependence from the measured I-V characteristics (Fig. 7.5) for parallel and antiparallel orientations of the ferromagnetic electrodes as shown in Fig. 7.7 (b) which result in similar values as those obtained from magnetoresistance hysteresis measurements.

Temperature dependence of tunnel junction resistance

The temperature dependence of the TMR as a function of bias voltage is measured. We observe that the TMR decreases quickly with an increase in temperature and is measurable upto only 180 K. It indicates that the curie temperature of the film close to interface of $SrTiO_3$ is close to 180 K. This is a common feature observed in manganite based junctions [4]-[9]. The two principal mechanisms that could explain the temperature dependence of the TMR: spin-flip scattering of tunneling electrons from impurities in the barrier or a reduction of the magnetic moment in the ferromagnet due to excitation of magnons. In LSMO, it is known that at the interface the magnetization is suppressed, which might cause lower T_C.

As compared to LSMO/$SrTiO_3$/LSMO junctions reported in the literature, we have obtained lower TMR vales. Factors like non-ideal tunnel barriers, lowering of magnetization at FM/I interface might result in such values. TMR values for our junctions can be enhanced further by improving the quality of the $SrTiO_3$ barrier, engineering the interfaces between the FM electrodes and $SrTiO_3$ in order to obtain high TMR values, hence high spin polarization in these junctions.

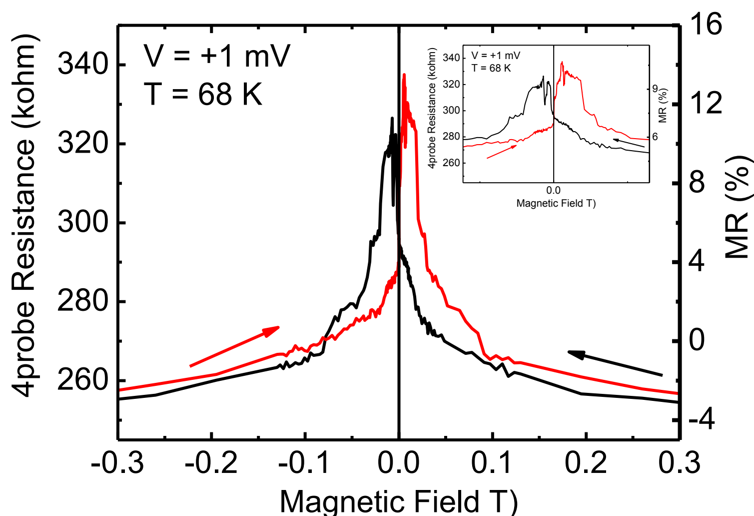

Figure 7.6: *Field dependent tunnel magnetoresistance at 68 K as a function of applied external magnetic field in a direction in plane to the sample. A maximum values of 14% is obtained using the formula shown in inset.*

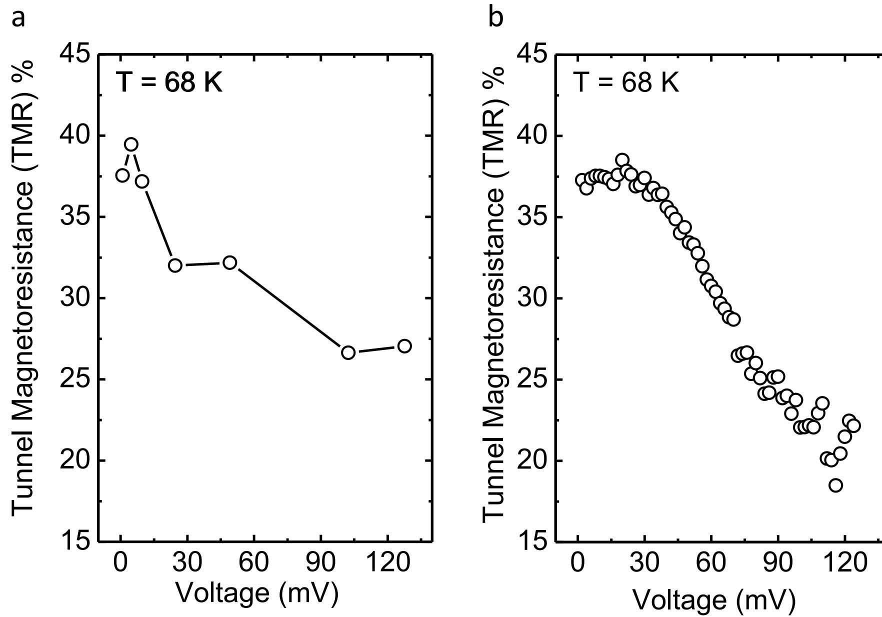

Figure 7.7: *Bias dependence of tunnel magnetoresistance at 68 K obtained for the parallel (P) and antiparallel (AP) alignments of electrode magnetizations for the LSMO. (a) Individual MR hysteresis are measured. (b) I-V shown in Fig. 7.5 is used to obtain bias dependent MR values.*

7.4 Conclusion

In conclusion, we have fabricated a all-oxide magnetic heteroepitaxial tunnel junctions using pulsed laser deposition, where LSMO is used as a ferromagnet and $SrTiO_3$ as the tunnel barrier. Electrical characterization of the tunnel barrier is presented. Our initial results of TMR measurements in all oxide magnetic tunnel junctions show a 36% of TMR at 68 K and 1 mV. Usual reduction of TMR with applied bias as well as increase in temperature is observed. Certainly, higher TMR values can be obtained by implementing the discussed factors. Further, such successful MTJ fabrication along with our understanding about hot electron transport in LSMO, is a step towards studying all oxide based magnetic tunnel transistors.

Bibliography

[1] E. Y. Tsymbal and D. G. Pettifor, Modelling of spin-polarized electron tunnelling from 3d ferromagnets. *J. Phys. Condens. Matter.* **9**, L411 (1997).

[2] C. Kaiser, S. van Dijken, S.-H. Yang, H. Yang, and S. S. P. Parkin, Role of tunneling matrix elements in determining the magnitude of the tunneling spin polarization of 3d transition metal ferromagnetic alloys. *Phys. Rev. Lett.* **94,** 247203 (2005).

[3] M. Bowen, M. Bibes, A. Barthélémy, J. P. Contour, A. Anane, Y. Lemaitre and A. Fert, Nearly total spin polarization in $La_{2/3}$ Sr $_{1/3}$ MnO_3 from tunneling experiments. *Appl. Phys. Lett.* **82,** 233-235 (2003).

[4] M. Viret, L. Ranno, and J. M. D. Coey, Magnetic localization in mixed-valence manganites. *Phys. Rev. B* **55,** 8067 (1997); M. Viret, M. Drouet, J. Nassar, J. P. Contour, C. Fermon and A. Fert, Low-field colossal magnetoresistance in manganite tunnel spin valves. *Europhys. Lett.* **39,** 545 (1997).

[5] J.-M De Teresa, A. Barthelemy, A. Fert, J.-P. Contour, F. Montaigne, P. Seneor, Role of Metal-Oxide Interface in Determining the Spin Polarization of Magnetic Tunnel Junctions. *Science* **286.** 507 (1999).

[6] A. Fert *et al.*, Review of recent results on spin polarized tunneling and magnetic switching by spin injection. *Materials. Sci. Engineering B* **84,** 1 (2001).

[7] J. S. Noh, T. K. Nath, C. B. Eom, J. Z. Sun, W. Tian, X. Q. Pan, Magnetotransport in manganite trilayer junctions grown by 90° off-axis sputtering. *Appl. Phys. Lett.* **79,** 233 (2001).

[8] Y. Lu, X.W. Li, G.Q. Gong, Gang Xiao, A. Guptaz, P.Lecoeur, J.Z. Sun, Y.Y. Wang, V.P. Dravid, Large magnetotunneling effect at low magnetic fields in micrometer-scale epitaxial $La_{0.67}Sr_{0.33}MnO_3$ tunnel junctions. *Phys. Rev. B* **54,** 8357 (1996).

[9] M. Bibes, Ll. Balcells, S. Valencia, S. Sena, B. Martinez, J. Fontcuberta, Thickness dependence of surface roughness and transport properties of $La_{2/3}$C $a_{1/3}MnO_3$ epitaxial thin films. *J. of Appl. Phys.* **89,** 6686 (2001).

[10] J. Bardeen. Tunneling from a Many-Particle Point of View. *Phys. Rev. Lett.* **6,** 57, (1961).

[11] H. Yamada, Y. Ogawa, Y. Ishii, H. Sato, M. Kawasaki, H. Akoh, and Y. Tokura, Engineered Interface of Magnetic Oxides. *Science* **305,** 5684, (2004).

[12] Y. Ishii, H. Yamada, H. Sato, H. Akoh, Y. Ogawa, M. Kawasaki, and Y. Tokura, Improved tunneling magnetoresistance in interface engineered (La,Sr)MnO_3 junctions. *Appl. Phys. Lett.* **4,** 89 (2006).

[13] A.H. Davis and J.M. MacLaren, Spin dependent tunneling at finite bias. *J. Appl. Phys.* **87,** 52247 (2000).

[14] Julliere, Tunneling between ferromagnetic films. *Phys. Lett.*, **54A,** 225 (1975).

[15] P. M. Tedrow and R. Meservey, Direct observation of spin-state mixing in superconductors. *Phys. Rev. Lett.* **27,** 919 (1971).

[16] Martinez, J.C. Ousset, J. Fontcuberta, ,Magnetotransport properties of fully strained epitaxial thin films of $La_{2/3}Ca_{1/3}MnO_3$ grown on $SrTiO_3$. *Appl. Surf. Sci.* **188,** 202 (2002).

[17] R. J. M. van de Veerdonk, J. Nowak, R. Meservey, J. S. Moodera, and W.J. M. de Jonge, Current distribution effects in magnetoresistive tunnel junctions. *Appl. Phys. Lett.* **71,** 2839 (1997).

[18] S. Zhang, P. M. Levy, A. C. Marley, and S. S. P. Parkin, Quenching of Magnetoresistance by Hot electrons in magnetic tunnel junctions. *Phys. Rev. Lett.* **79,** 3744 (1997).

[19] J. Zhang and R. M. White, Voltage dependence of magnetoresistance in spin dependent tunneling junctions. *J. Appl. Phys.* **83,** 6512 (1998).

[20] J. Z. Sun, D. W. Abraham, K. Roche, and S. S. P. Parkin, Temperature and bias dependence of magnetoresistance in doped manganite thin film trilayer junctions. *Phys. Lett.* 73, 1008 (1998); J. Z. Sun, L. Krusin Elbaum, P. R. Duncombe, A. Gupta, and R. B. Laibowitz, Temperature dependent, non-ohmic magnetoresistance in doped perovskite manganate trilayer junctions. *Appl. Phys. Lett.* **70,** 1769 (1997).